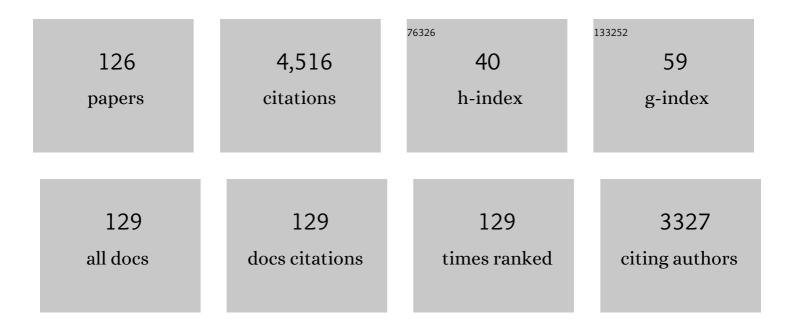
Balaram Sahoo

List of Publications by Year in descending order

Source: https://exaly.com/author-pdf/3377478/publications.pdf Version: 2024-02-01



#	Article	IF	CITATIONS
1	Collective Lamb Shift in Single-Photon Superradiance. Science, 2010, 328, 1248-1251.	12.6	338
2	Electromagnetically induced transparency with resonant nuclei in a cavity. Nature, 2012, 482, 199-203.	27.8	174
3	Carbon encapsulated nanoscale iron/iron-carbide/graphite particles for EMI shielding and microwave absorption. Physical Chemistry Chemical Physics, 2017, 19, 23268-23279.	2.8	148
4	Correlated vibrations of the tetrahedral and octahedral complexes and splitting of the absorption bands in FTIR spectra of Li-Zn ferrites. Vibrational Spectroscopy, 2017, 92, 267-272.	2.2	112
5	Observation of phase transformations in cement during hydration. Construction and Building Materials, 2015, 101, 122-129.	7.2	108
6	Effect of Zn substitution on the structural and magnetic properties of nanocrystalline NiFe2O4 ferrites. Ceramics International, 2018, 44, 4946-4954.	4.8	90
7	Graphene-oxide coating for corrosion protection of iron particles in saline water. Carbon, 2018, 140, 477-487.	10.3	90
8	Observation of enhanced magnetic pinning in Sm3+ substituted nanocrystalline Mn Zn ferrites prepared by propellant chemistry route. Journal of Alloys and Compounds, 2016, 682, 263-274.	5.5	75
9	Combustion synthesis, structure and magnetic properties of Li-Zn ferrite ceramic powders. Ceramics International, 2017, 43, 14431-14440.	4.8	71
10	Composition dependent elastic and thermal properties of Li Zn ferrites. Journal of Alloys and Compounds, 2017, 728, 1091-1100.	5.5	68
11	Impedance spectroscopic study on microwave sintered (1 â^' x) Na0.5Bi0.5TiO3–x BaTiO3 ceramics. Jo of Materials Science: Materials in Electronics, 2018, 29, 6966-6977.	ournal 2.2	67
12	Effect of morphology and role of conductivity of embedded metallic nanoparticles on electromagnetic interference shielding of PVDF-carbonaceous-nanofiller composites. Carbon, 2020, 164, 357-368.	10.3	67
13	Effect of the band gap and the defect states present within band gap on the non-linear optical absorption behaviour of yttrium aluminium iron garnets. Optical Materials, 2020, 108, 110163.	3.6	62
14	Annealing temperature dependent structural and magnetic properties of MnFe 2 O 4 nanoparticles grown by sol-gel auto-combustion method. Journal of Magnetism and Magnetic Materials, 2017, 433, 29-34.	2.3	61
15	Thermally induced phase transformation in multi-phase iron oxide nanoparticles on vacuum annealing. Journal of Magnetism and Magnetic Materials, 2017, 439, 156-166.	2.3	61
16	Application of monodisperse Fe3O4 submicrospheres in magnetorheological fluids. Journal of Industrial and Engineering Chemistry, 2018, 67, 347-357.	5.8	59
17	Low temperature dielectric properties and NTCR behavior of the BaFe _{0.5} Nb _{0.5} O ₃ double perovskite ceramic. Physical Chemistry Chemical Physics, 2020, 22, 2986-2998.	2.8	58
18	Enhancing absorption dominated microwave shielding in Co@C–PVDF nanocomposites through improved magnetization and graphitization of the Co@C-nanoparticles. Physical Chemistry Chemical Physics, 2019, 21, 15595-15608.	2.8	57

#	Article	IF	CITATIONS
19	Composition dependent structural and morphological modifications in nanocrystalline Mn-Zn ferrites induced by high energy Î ³ -irradiation. Materials Chemistry and Physics, 2017, 199, 313-321.	4.0	55
20	Modulating non-linear optical absorption through controlled graphitization of carbon nanostructures containing Fe3C-graphite core-shell nanoparticles. Carbon, 2019, 153, 545-556.	10.3	55
21	Synthesis of nanocrystalline spinel ferrite (MFe2O4, MÂ= Zn and Mg) by solution combustion method: Influence of fuel to oxidizer ratio. Journal of Alloys and Compounds, 2018, 742, 577-586.	5.5	54
22	Effect of Microstructure and Magnetic Properties of Ba-Pb-Hexaferrite Particles on EMI Shielding Behavior of Ba-Pb-Hexaferrite-Polyaniline-Wax Nanocomposites. Journal of Electronic Materials, 2020, 49, 1618-1629.	2.2	54
23	Mechanism of Î ³ -irradiation induced phase transformations in nanocrystalline Mn0.5Zn0.5Fe2O4 ceramics. Journal of Solid State Chemistry, 2017, 246, 119-124.	2.9	51
24	Evidence of structural damage in Sm and Gd co-doped Mn–Zn ferrite ceramics due to high-energy gamma irradiation. Ceramics International, 2016, 42, 15933-15939.	4.8	49
25	Nitrogen doping as a fundamental way to enhance the EMI shielding behavior of cobalt particle-embedded carbonaceous nanostructures. New Journal of Chemistry, 2019, 43, 5568-5580.	2.8	49
26	Ni Nanoparticles Coated with Nitrogen-Doped Carbon for Optical Limiting Applications. ACS Applied Nano Materials, 2020, 3, 8618-8631.	5.0	49
27	Structural and Magnetic Phase Transformations of Hydroxyapatite-Magnetite Composites under Inert and Ambient Sintering Atmospheres. Journal of Physical Chemistry C, 2015, 119, 6539-6555.	3.1	48
28	Mechanistic Insight into the Critical Concentration of Barium Hexaferrite and the Conductive Polymeric Phase with Respect to Synergistically Electromagnetic Interference (EMI) Shielding. ChemistrySelect, 2017, 2, 830-841.	1.5	47
29	Synthesis of coral-shaped yttrium-aluminium-iron garnets by solution-combustion method. Ceramics International, 2018, 44, 3024-3031.	4.8	47
30	Graphene Oxide Coatings on Amino Acid Modified Fe Surfaces for Corrosion Inhibition. ACS Applied Nano Materials, 2020, 3, 3540-3557.	5.0	47
31	Effect of Coralâ€5haped Yttrium Iron Garnet Particles on the EMI Shielding Behaviour of Yttrium Iron Garnetâ€Polyanilineâ€Wax Composites. ChemistrySelect, 2018, 3, 2120-2130.	1.5	46
32	Structural transformations and physical properties of (1  â²â€‰â€‰ <i>x</i>) Na _{0.5} Bi _{0.5} TiO ₃ ⰳ  ci>x BaTiO ₃ solic a morphotropic phase boundary. Journal of Physics Condensed Matter, 2019, 31, 075401.	d s ola tions	s n ea r
33	Magnetic interactions in water based ferrofluids studied by Mössbauer spectroscopy. Journal of Physics Condensed Matter, 2007, 19, 016205.	1.8	44
34	Application of Ni-Zn ferrite powders with polydisperse spherical particles in magnetorheological fluids. Powder Technology, 2018, 338, 190-196.	4.2	44
35	Effect of Sr-doping on sinterability, morphology, structure, photocatalytic activity and AC conductivity of ZnO ceramics. Journal of Materials Science: Materials in Electronics, 2017, 28, 13587-13595.	2.2	43
36	Structural, optical and M¶ssbauer spectroscopic investigations on the environment of Fe in Fe-doped ZnO (Zn1-xFexO) ceramics synthesized by solution combustion method. Ceramics International, 2019, 45, 24625-24634.	4.8	43

#	Article	IF	CITATIONS
37	Role of oxygen functionalities of GO in corrosion protection of metallic Fe. Carbon, 2021, 173, 350-363.	10.3	43
38	Magnetic and catalytic properties of Cu-substituted SrFe12O19 synthesized by tartrate-gel method. Advanced Powder Technology, 2020, 31, 2385-2393.	4.1	42
39	Effect of Mg-substitution in Co–Ni-Ferrites: Cation distribution and magnetic properties. Materials Chemistry and Physics, 2020, 251, 123081.	4.0	42
40	Mössbauer spectroscopic investigations of nanophase iron oxides synthesized by thermal plasma route. Materials Characterization, 2008, 59, 1215-1220.	4.4	41
41	Magnetorheological fluids containing rod-shaped lithium–zinc ferrite particles: the steady-state shear response. Soft Matter, 2018, 14, 5407-5419.	2.7	41
42	Investigation on structural, Mössbauer and ferroelectric properties of (1â^'x)PbFe0.5Nb0.5O3–(x)BiFeO3 solid solution. Journal of Magnetism and Magnetic Materials, 2016, 418, 122-127.	2.3	40
43	Role of pyrolysis reaction temperature and heating-rate in the growth and morphology of carbon nanostructures. Nano Structures Nano Objects, 2017, 12, 229-238.	3.5	40
44	Effect of annealing temperature on the structural and magnetic properties of Ba-Pb-hexaferrite powders synthesized by sol-gel auto-combustion method. Ceramics International, 2018, 44, 8877-8889.	4.8	40
45	Investigation of disorder in carbon encapsulated core-shell Fe/Fe3C nanoparticles synthesized by one-step pyrolysis. Diamond and Related Materials, 2018, 90, 62-71.	3.9	40
46	Infrared photodetectors based on multiwalled carbon nanotubes: Insights into the effect of nitrogen doping. Applied Surface Science, 2021, 538, 148187.	6.1	40
47	Investigation of structural, morphological and NTCR behaviour of Cu-doped ZnO nanoceramics synthesized by high energy ball milling. Materials Chemistry and Physics, 2019, 221, 419-429.	4.0	39
48	Mechanistic insights into the sol-gel synthesis of complex (quaternary) Co–Mn–Zn-spinel ferrites: An annealing dependent study. Ceramics International, 2020, 46, 17400-17415.	4.8	39
49	Changes in ferromagnetic spin structure induced by exchange bias in Fe/MnF2films. Physical Review B, 2004, 70, .	3.2	38
50	Strain induced magnetism and superexchange interaction in Cr substituted nanocrystalline cobalt ferrite. Materials Chemistry and Physics, 2018, 211, 54-64.	4.0	38
51	Comparative study of the structural and magnetic properties of alpha and beta phases of lithium ferrite nanoparticles synthesized by solution combustion method. Journal of Magnetism and Magnetic Materials, 2018, 462, 136-143.	2.3	38
52	Magnetic and ferroelectric characteristics of Gd 3 + and Ti 4 + co-doped BiFeO 3 ceramics. Bulletin of Materials Science, 2016, 39, 593-601.	1.7	37
53	One-step pyrolytic synthesis and growth mechanism of coreat shell type Fe/Fe <mmi:math xmlns:mml="http://www.w3.org/1998/Math/MathML" id="mml11" display="inline" overflow="scroll" altimg="si11.gif"><mml:msub><mml:mrow /><mml:mrow><mml:mn>3</mml:mn></mml:mrow></mml:mrow </mml:msub>C-graphite</mmi:math 	3.5	37
54	nanoparticles-embedded carbon globules. Nano Structures Nano Objects, 2018, 16, 77-85. Magnetic field dependent steady-state shear response of Fe ₃ O ₄ micro-octahedron based magnetorheological fluids. Physical Chemistry Chemical Physics, 2018, 20, 20247-20256.	2.8	36

#	Article	IF	CITATIONS
55	FeCoCr alloy-nanoparticle embedded bamboo-type carbon nanotubes for non-linear optical limiting application. Journal of Alloys and Compounds, 2020, 849, 156665.	5.5	36
56	Mechanistic insights into the optical limiting performance of carbonaceous nanomaterials embedded with core–shell type graphite encapsulated Co nanoparticles. Physical Chemistry Chemical Physics, 2020, 22, 27224-27240.	2.8	35
57	Synthesis, characterization and catalytic properties of trivalent iron substituted hexagonal mesoporous aluminophosphatesElectronic supplementary information (ESI) available: XRD patterns. See http://www.rsc.org/suppdata/cc/b2/b204215k/. Chemical Communications, 2002, , 1466-1467.	4.1	33
58	Cation distributions and magnetism of Al-substituted CoFe2O4 - NiFe2O4 solid solutions synthesized by sol-gel auto-combustion method. Ceramics International, 2018, 44, 20708-20715.	4.8	33
59	Structural, magnetic and M¶ssbauer studies on nickel-zinc ferrites synthesized via a precipitation route. Physica Status Solidi C: Current Topics in Solid State Physics, 2004, 1, 3495-3498.	0.8	32
60	Effect of solvents on the structure and magnetic properties of pyrolysis derived carbon globules embedded with iron/iron carbide nanoparticles and their applications in magnetorheological fluids. Nano Structures Nano Objects, 2018, 16, 167-173.	3.5	31
61	Steady-shear magnetorheological response of fluids containing solution-combustion-synthesized Ni-Zn ferrite powder. Advanced Powder Technology, 2018, 29, 2188-2193.	4.1	31
62	Structural and magnetic properties of Al-doped yttrium iron garnet ceramics: 57Fe internal field NMR and Mössbauer spectroscopy study. Journal of Alloys and Compounds, 2019, 773, 612-622.	5.5	31
63	Composition dependent room temperature structure, electric and magnetic properties in magnetoelectric Pb(Fe 1/2 Nb 1/2)O 3 Pb(Fe 2/3 W 1/3)O 3 solid-solutions. Journal of Alloys and Compounds, 2016, 677, 27-37.	5.5	30
64	Magneto-mechanical response of additive-free Fe-based magnetorheological fluids: role of particle shape and magnetic properties. Materials Research Express, 2018, 5, 085703.	1.6	30
65	Dose dependent modifications in structural and magnetic properties of γ-irradiated nanocrystalline Mn0.5Zn0.5Fe2O4 ceramics. Ceramics International, 2017, 43, 523-526.	4.8	29
66	Studies of ferroelectric properties and leakage current behaviour of microwave sintered ferroelectric Na _{0.5} Bi _{0.5} TiO ₃ ceramic. Ferroelectrics, 2017, 517, 25-33.	0.6	28
67	Determination of magnetic domain state of carbon coated iron nanoparticles via 57Fe zero-external-field NMR. Journal of Magnetism and Magnetic Materials, 2018, 453, 125-131.	2.3	28
68	Tuning the fluorescence behavior of liquid crystal molecules containing Schiff-base: Effect of solvent polarity. Journal of Luminescence, 2019, 210, 371-375.	3.1	27
69	Carbon nanotubes or carbon globules: Optimization of the pyrolytic synthesis parameters and study of the magnetic properties. Nano Structures Nano Objects, 2018, 14, 131-137.	3.5	26
70	High-energy phonon confinement in nanoscale metallic multilayers. Physical Review B, 2008, 77, .	3.2	25
71	57Fe internal field nuclear magnetic resonance and Mössbauer spectroscopy study of Li-Zn ferrites. Journal of Magnetic Resonance, 2018, 286, 68-77.	2.1	25
72	Effect of magnetic dipolar interactions and size dispersity on the origin of steady state magnetomechanical response in bidisperse Mn–Zn ferrite spherical particle based magnetorheological fluids. New Journal of Chemistry, 2019, 43, 9969-9979.	2.8	25

#	Article	IF	CITATIONS
73	Synthesis of highly magnetic Mn-Zn ferrite (Mn0.7Zn0.3Fe2O4) ceramic powder and its use in smart magnetorheological fluid. Rheologica Acta, 2019, 58, 273-280.	2.4	25
74	Origin of room temperature weak-ferromagnetism in antiferromagnetic Pb(Fe2/3W1/3)O3 ceramic. Ceramics International, 2015, 41, 11680-11686.	4.8	24
75	Direct measurement of depth-dependent Fe spin structure during magnetization reversal in <mml:math xmlns:mml="http://www.w3.org/1998/Math/MathML" display="inline"><mml:mrow><mml:mtext>Fe</mml:mtext><mml:mo>/</mml:mo><mml:msub><mml:mrow> bilavers. Physical Review B. 2008. 78.</mml:mrow></mml:msub></mml:mrow></mml:math 	<mml:mtex< td=""><td>t>MnF</td></mml:mtex<>	t>MnF
76	Solvent dependent morphology and ⁵⁹ Co internal field NMR study of Co-aggregates synthesized by a wet chemical method. Physical Chemistry Chemical Physics, 2018, 20, 17739-17750.	2.8	22
77	Steady-shear response of magnetorheological fluid containing coral-shaped yttrium-iron-garnet particles. Materials Research Bulletin, 2019, 113, 45-50.	5.2	22
78	Tunable Dielectric Properties of Nickel Ferrite Derived via Crystallographic Site Preferential Cation Substitution. Journal of Physical Chemistry C, 2022, 126, 9123-9134.	3.1	22
79	On the Room Temperature Ferromagnetic and Ferroelectric Properties of Pb(Fe1/2Nb1/2)O3. Journal of Superconductivity and Novel Magnetism, 2015, 28, 2465-2472.	1.8	21
80	Role of iron in the enhanced reactivity of pulverized Red mud: Analysis by Mössbauer spectroscopy and FTIR spectroscopy. Case Studies in Construction Materials, 2019, 11, e00266.	1.7	21
81	Role of Mg ²⁺ and In ³⁺ substitution on magnetic, magnetostrictive and dielectric properties of NiFe ₂ O ₄ ceramics derived from nanopowders. Physical Chemistry Chemical Physics, 2021, 23, 1694-1705.	2.8	21
82	EMI shielding performance of lead hexaferrite/polyaniline composite in 8-18â€GHz frequency range. AIP Conference Proceedings, 2018, , .	0.4	20
83	Synthesis, composition and spin-dynamics of FCC and HCP phases of pyrolysis derived Co-nanoparticles embedded in amorphous carbon matrix. Ceramics International, 2019, 45, 19879-19887.	4.8	20
84	Chemically enabling CoFe2O4 for magnetostrictive strain sensing applications at lower magnetic fields: Effect of Zn substitution. Materials Science and Engineering B: Solid-State Materials for Advanced Technology, 2021, 266, 115080.	3.5	20
85	XRD, internal field-NMR and Mössbauer spectroscopy study of composition, structure and magnetic properties of iron oxide phases in iron ores. Journal of Materials Research and Technology, 2019, 8, 2192-2200.	5.8	19
86	Gamma-irradiation induced modifications in structural and magnetic properties of nanocrystalline Mn0.5Zn0.5 SmxFe2-xO4 ceramics. Radiation Physics and Chemistry, 2020, 166, 108506.	2.8	19
87	Atomic vibrational dynamics of amorphous Fe–Mg alloy thin films. Journal of Physics and Chemistry of Solids, 2005, 66, 2263-2270.	4.0	18
88	Strengthening mechanisms in Fe-Al based ferritic low-density steels. Materials Science & Engineering A: Structural Materials: Properties, Microstructure and Processing, 2018, 712, 574-584.	5.6	18
89	Role of graphitization-controlled conductivity in enhancing absorption dominated EMI shielding behavior of pyrolysis-derived Fe3C@C-PVDF nanocomposites. Materials Chemistry and Physics, 2021, 263, 124429.	4.0	18
90	Enabling cobalt ferrite (CoFe2O4) for low magnetic field strain responsivity through Bi3+ substitution: Material for magnetostrictive sensors. Journal of Alloys and Compounds, 2021, 877, 160285.	5.5	17

#	Article	IF	CITATIONS
91	Fe–Cu granular thin films with giant magnetoresistance by thermionic vacuum arc method: Preparation and structural characterization. Surface and Coatings Technology, 2005, 200, 980-983.	4.8	16
92	Enhancing functional properties of PVDF-HFP/BZT-BCT polymer-ceramic composites by surface hydroxylation of ceramic fillers. Ceramics International, 2021, 47, 33563-33576.	4.8	16
93	Magnetic Properties of MFeCrO4 (M = Co/Ni) Prepared by Solution Combustion Method. Journal of Superconductivity and Novel Magnetism, 2019, 32, 2973-2979.	1.8	14
94	Atomic vibrational density of states in crystalline and amorphous Tb1ÂxFexalloy thin films studied by nuclear resonant inelastic x-ray scattering (NRIXS). Journal of Physics Condensed Matter, 2004, 16, S379-S393.	1.8	13
95	Excited state intramolecular proton transfer emission in bent core liquid crystals. Journal of Photochemistry and Photobiology A: Chemistry, 2018, 358, 186-191.	3.9	13
96	Evidence for Room-Temperature Weak Ferromagnetic and Ferroelectric Ordering in Magnetoelectric Pb(Fe0.634W0.266Nb0.1)O3 Ceramic. Journal of Superconductivity and Novel Magnetism, 2017, 30, 1317-1325.	1.8	12
97	Exploring supercapacitance of solvothermally synthesized N-rGO sheet: role of N-doping and the insight mechanism. Physical Chemistry Chemical Physics, 2022, 24, 1059-1071.	2.8	12
98	Title is missing!. Hyperfine Interactions, 2002, 144/145, 65-76.	0.5	11
99	Mössbauer spectroscopical investigation of the exchange biased Fe/MnF2 interface. Hyperfine Interactions, 2007, 169, 1371-1377.	0.5	11
100	Effect of fuel and fuel to oxidizer ratio in solution combustion synthesis of nanoceramic powders: MgO, CaO and ZnO. Solid State Sciences, 2020, 109, 106426.	3.2	11
101	Role of Composition in Enhancing Heat Transfer Behavior of Carbon Nanotube-Ethylene Glycol Based Nanofluids. Electronic Materials Letters, 2020, 16, 595-603.	2.2	11
102	Sol-gel auto-combustion synthesis of Ba–Sr hexaferrite ceramic powders. Ceramics International, 2021, 47, 14907-14912.	4.8	10
103	Sensing of oxidizing and reducing gases by sensors prepared using nanoscale Co3O4 powders: A study through Cu substitution. Advanced Powder Technology, 2022, 33, 103529.	4.1	10
104	MÂssbauer effect study of the Fe spin structure in exchange-bias and exchange-spring systems. Journal Physics D: Applied Physics, 2002, 35, 2352-2358.	2.8	9
105	Structural and magnetic properties of iron species/SiO2 nanocomposites obtained by sol-gel methods. Physica Status Solidi C: Current Topics in Solid State Physics, 2004, 1, 3507-3510.	0.8	9
106	One-step synthesis of diopside (CaMgSi2O6) ceramic powder by solution combustion method. Advanced Powder Technology, 2020, 31, 3492-3499.	4.1	9
107	Micro-mechanism of evolution of microstructure and texture in Ni-Fe alloys. Materialia, 2020, 13, 100811.	2.7	9
108	Superiority of graphite coated metallic-nanoparticles over graphite coated insulating-nanoparticles for enhancing EMI shielding. New Journal of Chemistry, 2021, 45, 4592-4600.	2.8	9

#	Article	IF	CITATIONS
109	Dielectric properties of A-site Mn-doped bismuth sodium titanate perovskite: (Bi0·5Na0.5)0.9Mn0·1TiO3. Materials Chemistry and Physics, 2021, 270, 124849.	4.0	9
110	Crystal growth and effect of defects on the dielectric properties of ammonium dihydrogen phosphate (ADP) single crystals. Journal of Materials Science: Materials in Electronics, 2020, 31, 10548-10552.	2.2	8
111	Preparation and structural investigation of epitaxially grown antiferromagnetic FeSn2(001) thin films on InSb(001). Journal of Applied Physics, 2003, 94, 3573-3581.	2.5	7
112	Magnetic interactions and spin configuration in FeRh and Fe/FeRh systems. Journal of Magnetism and Magnetic Materials, 2004, 272-276, 348-350.	2.3	5
113	Electronic transport and atomic vibrational properties of semiconducting Mg Sn thin film. Phase Transitions, 2006, 79, 839-852.	1.3	5
114	Superconductivity of MgB 2 Thin Films Prepared By CoEvaporation and Magnetism of MgB 2 /Fe Multilayers Studied By Mössbauer Spectroscopy. Phase Transitions, 2003, 76, 423-435.	1.3	3
115	Mössbauer spectroscopical investigation of amorphous Fe–Y alloy ribbons prepared by melt spinning. Hyperfine Interactions, 2007, 165, 175-181.	0.5	3
116	Preparation and Characterization of Ultrathin Stainless Steel Films. , 2011, , .		3
117	As-grown superconducting MgB2thin films prepared at extreme deposition conditions. Superconductor Science and Technology, 2012, 25, 015004.	3.5	3
118	Neutron diffraction, Mössbauer effect and electron paramagnetic resonance studies on multiferroic Pb(Fe2/3W1/3)O3. AIP Conference Proceedings, 2015, , .	0.4	3
119	Structure and magnetic properties of Ni substituted Co-Mg nanocrystal line ferrites synthesized by sol-gel auto-combustion method. AIP Conference Proceedings, 2020, , .	0.4	3
120	Amorphous Fe–Mg alloy thin films: magnetic properties and atomic vibrational dynamics. Hyperfine Interactions, 2007, 168, 1185-1190.	0.5	2
121	Amorphous Fe-Mg alloy thin films: magnetic properties and atomic vibrational dynamics. , 2006, , 1185-1190.		1
122	Vibrational dynamics of Fe in amorphous Fe–Sc and Fe–Al alloy thin films. Hyperfine Interactions, 2007, 170, 33-46.	0.5	1
123	Metallurgical phases and their magnetism at the interface of nanoscale MgB2/Fe layered structures. Journal of Physics Condensed Matter, 2011, 23, 475702.	1.8	1
124	Neutron diffraction, Mössbauer and electron paramagnetic resonance studies of Pb0.8Bi0.2Fe0.6Nb0.4O3 multiferroic. AIP Conference Proceedings, 2017, , .	0.4	1
125	Mössbauer spectroscopical investigation of the exchange biased Fe/MnF2 interface. , 2006, , 1371-1377.		1
126	Vibrational dynamics of Fe in amorphous Fe-Sc and Fe-Al alloy thin films. , 2006, , 33-46.		0